

DEFORMATION BEHAVIOUR OF STRUCTURES EXPOSED AT VERY HIGH TEMPERATURES TO CYCLIC THERMAL AND MECHANICAL LOADINGS

G. Breitbach¹, A. Schmidt-Plutka², F. Schubert¹ and H. Nickel¹

¹Institute of Reactor Materials, Research Center Juelich, Germany

²EMA Elektro-Maschinen, Schultze GmbH & Co. KG, D-6932 Hirschhorn/Neckar, Germany

Abstract:

At very high temperatures enhanced creep deformations may be produced by the superposition of load controlled stresses and cyclic thermal stresses (creep ratcheting). Thick walled tubes made from ALLOY 800 were loaded by an axial force at temperatures around 900°C. The inductive heating facility was cyclically operated in such a manner that in the tube walls temperature differences of 40 °C occurred. The axial elongation was measured. For comparison at the same specimen the elongation was also measured under constant temperatures (at the mean temperature of the cycle). Under cyclic conditions a larger elongation rate was observed. The ratcheting effect was clearly seen. The inelastic stress analysis using simple constitutive creep equations predicted a lower effect.

1. Introduction

Design and dimensioning of components for nuclear power plants are much more expensive and detailed in comparison to the conventional field. A lot of work is to do for the specification of expected loadings during the life time of the plant. Extreme situations and accidents are to take into account. The impacts of load cases are analysed often under very conservative boundary conditions, where phenomena are to take into account which are not considered in conventional design procedures. For the heat exchangers of the Helium Cooled High Temperature Reactor the creep ratcheting is such a phenomenon /1,2/. Under "creep ratcheting" an effect is understood where the creep strain accumulation is enhanced, if cyclic secondary stresses (strain controlled stresses) are superposed to the primary stresses (load controlled stresses). The risk of enhanced creep deformations was seen for the heat exchangers with projected temperature levels above 800°C, because more or less regular hot streaks of the heated fluids can produce cyclic thermal stresses in the tube walls.

2. The ratcheting phenomenon

With respect to the geometries and loading situations of the components the analysis of ratcheting requires a complicated calculation and modelling expense. However, the ratcheting phenomenon is a familiar experience. If a bar of a very ductile material is to lengthen it is possible to do it by pure pulling,

but it may be more effective beside the pulling to bend it up and down. A cyclic bending moment is superposed to the pulling force enhancing the lengthening. The moment acts like an amplifier for the force in producing elongation.

In tubes momentlike stress distributions are produced if a temperature gradient across the wall is established. The cold parts of the wall are found in tension since the hotter parts are compressed. In general load controlled axial and hoop stresses are superposed e.g. resulting from pressure loads. In case of the cyclical occurrence of the gradient a typical ratcheting situation is given.

For fuel cans of fast breeder reactors which are exposed to high heat fluxes with large temperature gradients and which have to withstand larger internal pressures caused by gaseous fission products, the ratcheting effect was discussed and investigated /3/. For the evaluation the Bree diagram was developed where the main emphasis was laid on the plastic ratcheting.

In Helium Cooled High Temperature Reactors the heat exchangers can be exposed to cyclic temperature conditions (e.g. start up, shut down, hot streaks of the fluids) leading to constrained thermal strains. The temperature level in the hottest parts is above 800 °C where creep phenomena are dominant. In addition mechanical loads are acting so that ratcheting has to be taken into consideration.

3. Experimental concept

For the experimental investigation of creep ratcheting thick walled tubes of ALLOY 800 were heated cyclically by an inductive heating facility at a temperature level of 900°C (Fig. 1). The electromagnetic frequency of the heating system was as high as 500 kHz so that, because of the skin effect, heat was produced by the induced currents only in a thin layer of the outer tube surface (around 100µm). This localisation of the heat source promoted the formation of inhomogeneous temperature states. Inside no heat sink was installed so that the inner surface of the tube could be regarded as being adiabatic. The temperature distribution of a typical heating cycle is shown in Fig. 2. This calculated results agreed very well with experimental measurements. In the case considered here a 10 second heating period was followed by a 10 second shut down phase. Cooling is caused mainly by heat radiation from the hot outer surface into the environment. A temperature curve like a sawtooth is observed at the outer surface in the range 880-920 °C under the chosen conditions. Inside the temperature oscillations are damped strongly.

The inhomogeneous temperature distribution results in thermal stresses. In Fig. 3 the axial thermal stress components calculated under elastic conditions are shown. On the outer and the inner surface tension and compression states change in an anticyclic manner. There is a stress range of nearly 80 MPa on the outer surface. Thus together with an induced outer load a ratcheting situation is given. During the experiment the load controlled stress was produced by an axial tension force.

The axial elongation of the tube was measured. For comparison after a period of cyclic conditions a period under constant temperatures (mean temperature of the cycle) followed. Subjected

to cyclic temperatures an enhanced elongation rate should occur because of creep ratcheting. Changing to constant temperatures it should decrease. The ratios of the elongation rates in the two sorts of experimental phases characterize the ratcheting effect.

4. Experimental results

The tubular specimens were heated to a temperature of 900 °C. The temperature constant zone was roughly 150 mm. Then the axial tension was induced via an actuator. An experiment of typical 1200 h duration was divided in time steps of some hundred hours during which cyclic or constant temperature conditions were applied. Fig. 4 shows the measured axial elongation of an experiment. The two nearby curves are obtained from readings of two extensometer arrangements. The axial primary stress was 25 MPa, the cyclic temperatures were according to Fig. 2. The first change to cyclic conditions occurred after 400 h. At every change from cyclic to constant temperatures remarkable changes of the elongation rates were observed. After longer times the elongation rates under creep ratcheting conditions were roughly 10 times larger than the rates at constant temperatures. In other experiments the chosen constant temperature level was the maximum cycle temperature (920°C). Here also under cyclic conditions higher rates occurred showing that the acceleration of elongation is not a pure temperature effect, but it results from the concurrence of cyclic induced secondary stresses and the axial primary stresses.

The typical experiment run to around 8% creep strain in the temperature constant zone. In the metallographic examinations no creep damage like voids or cracks could be observed though beside the creep deformations the outer surface was exposed to a remarkable fatigue loading.

5. Inelastic analysis of the creep ratcheting effect

Calculations of the stress strain behaviour were carried out using the FE-Code ABAQUS. The FE-mesh is shown in Fig. 5. The nodal points of the upper line are suppressed with respect to the axial direction whereas the points of the lower line are forced to move with the same displacement rate. That is the situation in a long tube under axisymmetric loading conditions away from the ends.

The modelling of creep especially under cyclic temperature conditions is not a simple task. Unified viscoplastic models are today more and more employed which relate the inelastic strain rate (creep, plasticity) to the stress state and to some internal variables, each obeying evolution equations /4,5/. However, for most materials suitable experimental data are not available. Most creep data are obtained by uniaxial constant load experiments at constant temperatures from which mostly a Norton-power law is derived /6/. Combining elasticity and power law creep a possible simple consistent constitutive equation in multiaxial formulation can be written as follows:

$$(1) \dot{\epsilon}_{ij} = \frac{1+\mu}{E} \cdot \dot{s}_{ij} + \frac{1-2\mu}{3E} \cdot \dot{s} \cdot \delta_{ij} + \frac{3}{2} \cdot k \cdot \sigma_e^{n-1} \cdot s_{ij}$$

Here the total strain rate, stress deviator and Kronecker's δ -components are denoted by $\dot{\epsilon}_{ij}$, s_{ij} and δ_{ij} respectively, s is the

trace of the stress tensor, σ_e the von Mises equivalent stress. E , μ are Young's modulus and Poisson's ratio respectively. The parameters k and n have been evaluated for ALLOY 800 from a lot of experiments resulting in the following expressions.

$$(2) \quad k(T) = 8.32 \cdot 10^{28} \cdot \exp\{-1.1 \cdot 10^5 / (T + 273.15)\} \quad \text{MPa}^{-n} \cdot \text{h}^{-1}$$

(T in °C)

$$(3) \quad n(T) = 13.5 - 5.82 \cdot 10^{-6} \cdot (T + 273.15)^2$$

The cyclic temperature fields according Fig.2 were taken as "thermal loadings" together with a load controlled axial stress of 25 MPa. As a result of the FE-analysis Fig. 6 shows the axial stress at the outer surface over 15 cycles. Comparing Fig. 6 and Fig. 3 it is seen that the stress response is practically an elastic one. The cycle time of 20 seconds is small compared to typical times during which remarkable creep deformations are generated ("rapid cyclic creep behaviour" /7/). But it does not mean that creep can be neglected. After a sufficient number of cycles a creep strain field is produced resulting in a stationary, cycle specific residual stress field superposed to the elastic response. Fig. 6 shows that the peak value of the tension stress decreases from cycle to cycle. The relaxation of this value is coupled with the development of the residual stress field.

The smoothed time course of the axial creep strains at three different positions of the wall is shown in Fig. 7. At the very beginning the creep strain at the outer surface increases rapidly. But from compatibility it is necessary that for longer times all curves have the same mean slope. For comparison the creep strain development according to the Norton law is shown for a uniaxial specimen at 25 MPa and 900 °C. The ratio of the slopes characterizes the ratcheting effect. It amounts here to a value between two and three. Fig. 7 also contains the course of the axial stress maximum at the outer surface (see also Fig. 6) drawn as a continuous curve. In approaching the quasistationary state the stress maximum converges against a limit value.

6. Comparison of theoretical and experimental results

The calculation of temperature fields was in a very good agreement with measured values. On the other hand the results obtained from the inelastic stress strain FE-analysis which led to an elongation rate ratio between two and three, were to subject to an evaluation. Beside the presented analysis based on the constitutive equation (1-3) further calculations were carried out varying the parameters of the Norton law. Enhancing the exponent n of the power law larger ratios in the range of five were obtained. It remained differences to the experimental results with ratios above 10. It should here be remarked that the Norton power law which is often used because of its simple structure, is not quite able to describe the behaviour under rapid cyclic loading conditions. Better but more complicated constitutive equations are the unified viscoplastic models with "Backstress parameters" as e.g. the Robinson or Chaboche Model /4,5/. But nevertheless the theoretical results obtained here

give an insight into the phenomenon and an indication of a clear enhancement of elongation rates under cyclic conditions.

References

- /1/ A. Schmidt-Plutka, "Verformungsverhalten dickwandiger Rohre aus X 10 NiCrAlTi 32 20 unter zyklischen thermomechanischen Beanspruchungen" Dissertation, RWTH Aachen (1992)
- /2/ R. Zottmaier, H. H. Over, F. Schubert, H. Nickel "Untersuchungen zum Kriechratcheting von Rohrproben", Forschungszentrum Jülich, Bericht Nr. 2019 (1985)
- /3/ J. Bree, Journal of Strain Analysis , Vol.2, No.3 (1967) 226-238
- /4/ D.N. Robinson, "A unified creep-plasticity model for structural metals at high temperature", ORNL Report/TM 5969, 1978
- /5/ J.L. Chaboche, Bull. Acad. Sciences, Serie Sciences Techniques, XXV, No.1, 33, (1977)
- /6/ H.J. Penkalla, "Die Werkstoffdatenbank der Entwicklungsgemeinschaft Hochtemperaturreaktor", VDI-Bericht Nr. 600.4 (1987)
- /7/ A.R.S. Ponter, Int. J. of Num. Meths. Eng., Vol. 12 (1978), 1001-1024

Figures

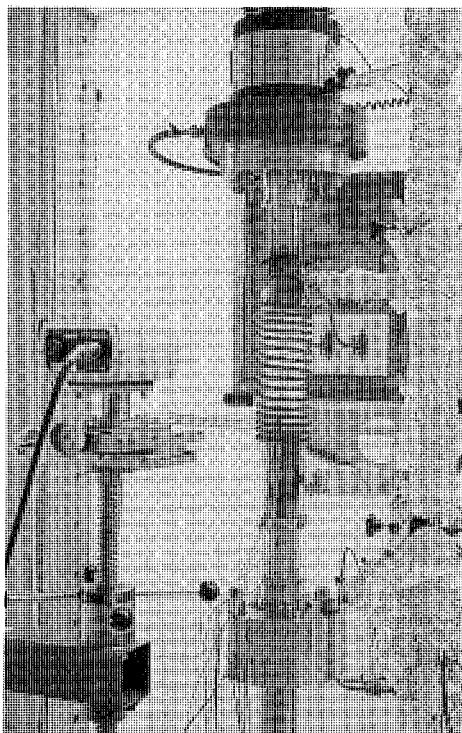


Fig. 1: Arrangement for creep experiments on inductive heated tube specimens (outer diameter 67mm, wall thickness 20mm) under constant and cyclic temperature conditions.

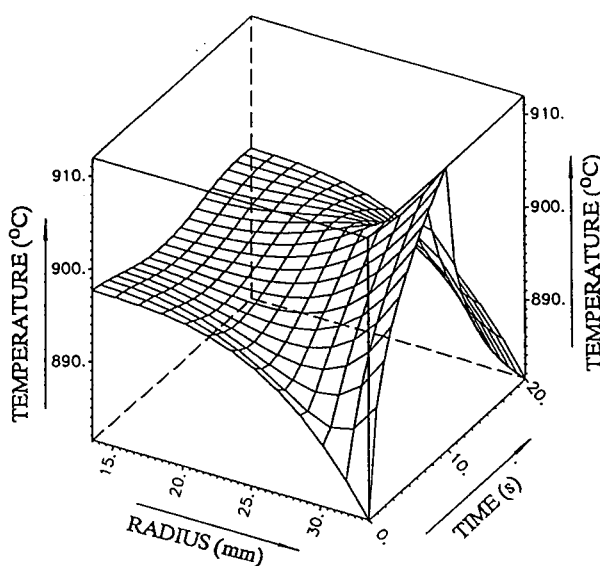


Fig. 2: Temperature cycle; 10 seconds heating of a thin surface layer, then shut down for 10 seconds; inner surface adiabatic, heat radiation at the outer surface into the environment.

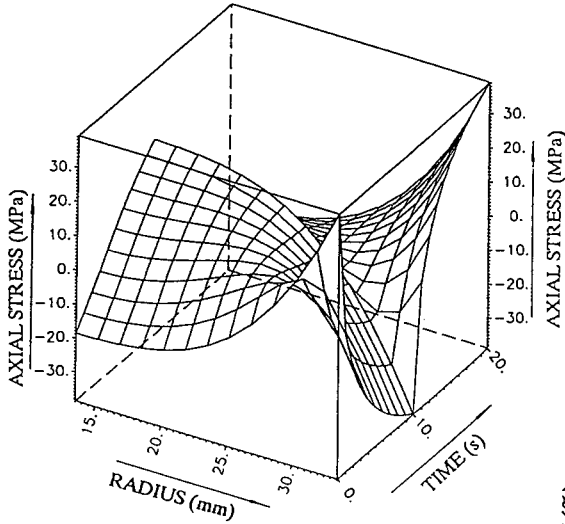


Fig. 3: Axial thermal stresses according to the temperature field of Fig. 5, elastic calculation.

Fig. 4: Axial strain based on two extensometer readings for the tube specimen BLY207; axial tension stress 25 MPa, changing periods of constant and cyclic temperatures; constant conditions during the phases 1,3,5,7,9,11 (900°C), cyclic conditions during the phases 2,4,6,8,10.

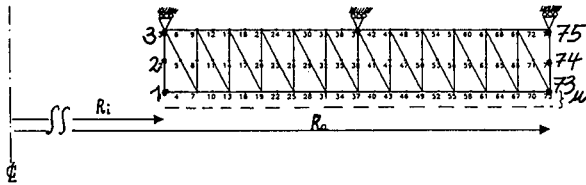
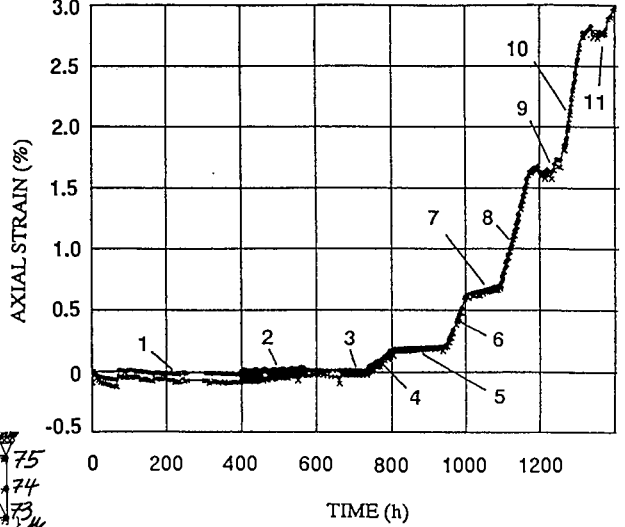


Fig. 5: FE-mesh(axisymmetric). Points 1,2,3 at $R_i=13,5\text{mm}$; points 73, 74, 75 at $R_o = 33,5\text{mm}$.

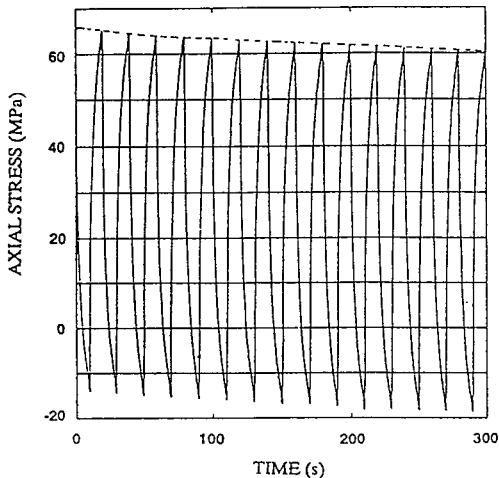


Fig. 6: Axial stress at the outer tube surface (15 cycles, FE-calculation)

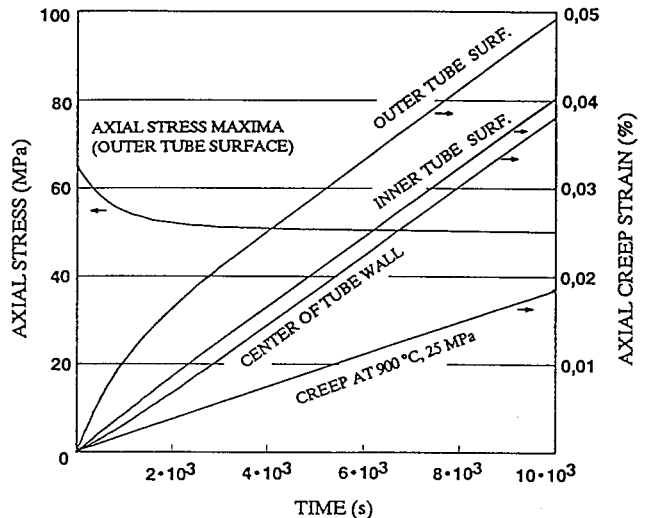


Fig.7: 3 smoothed curves of axial creep strains; creep strain course for 25 MPa, 900°C; continuous curve of the axial stress maximum at outer surface.